JOURNAL OF MATERIALS SCIENCE 11 (1976) 1939–1951

Fracture toughness and fracture of WC-Co composites

J. L. CHERMANT, F. OSTERSTOCK
Laboratoire de Chimie Minérale Industrielle, Groupe de Cristallographie et Chimie du Solide, L.A. 251 Université de Caen, 14032 Caen Cedex, France

Critical stress intensity factor, and related parameters have been measured in three-point bending for 18 different combinations of different volume fractions of cobalt (5 to 37%) and grain size of tungsten carbide (0.7, 1.1 and 2.2 μm). In particular, a study was made of the correlations between the strength and mechanical and microstructural parameters, such as $\bar{L}_{Co}$, C_{WC}, $\bar{L}_{Co}/\bar{D}_{WC}$, $\bar{L}^2_{Co}/\bar{D}_{WC}$, H_V and wear resistance. A hypothesis for the mechanism of fracture has been proposed following an analysis of these results and a study of the mode of fracture.

1. Introduction

A good knowledge of the mechanical characteristics of tungsten carbide–cobalt materials is necessary because their utilization is very often limited by their brittleness. This brittleness is accompanied by low toughness and extreme sensitivity to microstructural defects. Conventional mechanical tests have limited applicability. On the other hand, methods of fracture mechanics have been applied successfully to materials which are as brittle. Some measurements of the critical stress intensity factor, K_{IC}, already made on some WC–Co materials, show that the results are independent of the method used [1–6]. Furthermore one semi empirical model [7] and a qualitative model [4, 8] for the mechanism of fracture have been proposed. In this study we have applied these methods to specimens of different compositions and various grain sizes in order to obtain correlation between the critical stress intensity factor and the microstructural parameters such as are obtained from quantitative metallography and stereology.

2. Experimental procedure

2.1. Materials

The materials, WC–Co composites, employed were fabricated for us by Ugine–Carbone. They are divided in three ranges of mean diameter of tungsten carbide crystals (diameter of equivalent spheres) 2.2, 1.1 and 0.7 μm. The volume fraction of cobalt, $V_{V(Co)}$, varies between 5 and 37% (3 and 25 wt %).

The characteristic microstructural parameters were determined on optical or electron-optical micrographs depending on the mean diameter of the equivalent circle of the tungsten carbide crystals, from which the mean diameter of equivalent sphere was obtained, using the Saltykov corrections [9]. A minimum of 1500 crystals was counted [10]. The other microstructural parameters – mean free path in the cobalt phase, $\bar{L}_{Co}$, and contiguity of the carbide phase, C_{WC} – were obtained by the usual methods of linear analysis [11].

2.2. Specimen design and analysis

The specimens used for K_{IC} tests were 42 mm × 8 × 4 mm. They were squared off and pre-notched with a "V" or "U" with a diamond grinding wheel. The pre-notch was extended to a fine notch by spark erosion using a copper blade with a thickness 20 to 25 μm. The specimens were fractured in three-point bending in a Tinius Olsen machine, type Locap 100 000 N. The applied load was measured with a 1000 N load cell. The knife edges were in WC–Co (3% Co in wt), semicylindrical with a radius of curvature of 3 mm. The distance

between lower knife edges was 32 mm (Fig. 1). To conform to standards [12, 13] we have recorded the load applied as a function of the displacement across the notch at the specimen edge using a strain gauge extensometer. The signal from the extensometer is passed to an a.c. bridge Sedeme NS 45P, and from these to the abscissa of a Hewlett–Packard 7005-B recorder. The load is recorded on the ordinate.

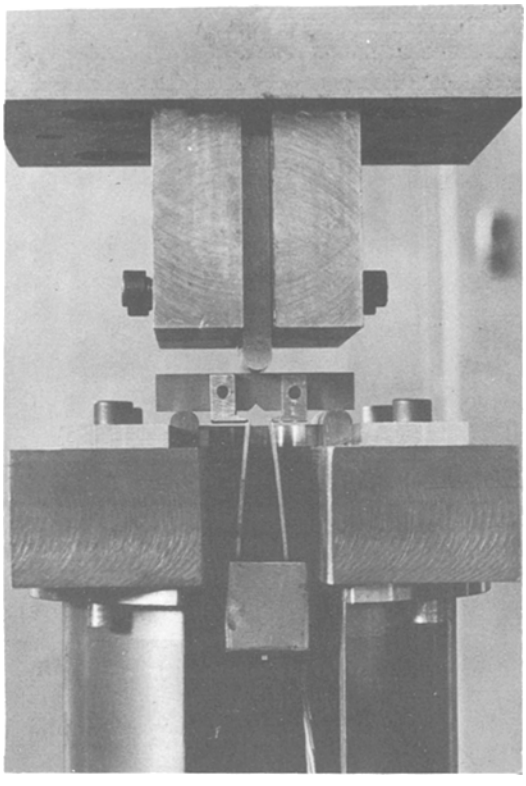

Figure 1 Arrangement of the K_{IC} equipment.

The values of K_{IC} were determined by the analytical method. The brittleness of WC–Co is such that a perfectly linear load displacement curve can be obtained (Fig. 2). In this case the value of K_{IC} can be obtained, knowing the rupture stress [14]:

$$K_{IC} = Y\sigma_r\sqrt{a}$$

In three-point bending this becomes:

$$K_{IC} = \frac{3F_rLY}{2le^2}\sqrt{a}$$

where F_r is the load at rupture, L the distance between lower knife edges, l the breadth of specimen, e the width of specimen, a the length of crack, and Y a form parameter which, in the case of three-point bending and $L/e \simeq 4$, is given by [14]:

$$Y = 1.93 - 3.07\left(\frac{e}{a}\right) + 14.53\left(\frac{e}{a}\right)^2 - 25.11\left(\frac{e}{a}\right)^3 + 25.80\left(\frac{e}{a}\right)^4$$

The critical value of the strain energy release rate, G_{IC}, is then given in the case of the plane strain by:

$$G_{IC} = \frac{K_{IC}^2}{E}(1-\nu^2)$$

where E is Young's modulus, and ν is Poisson's coefficient. We have taken $\nu = 0.2$ for the materials studied [15, 16]. The existence of a plastic zone at the crack tip imposes restrictions on the size of the specimen and the crack length, because it is necessary to ensure that a condition of plane strain is obtained and also that the strain cannot be relieved by general plastic deformation. These conditions are fulfilled if [12, 13]:

$$a \geqslant 2.5\left(\frac{K_{IC}}{\sigma_Y}\right)^2$$

$$l \geqslant 2.5\left(\frac{K_{IC}}{\sigma_Y}\right)^2.$$

We have calculated the size of the plastic zone using the approximation given by Irwin [17]. Its radius in the plane strain is given by:

$$r_Y = \frac{1}{6\pi}\left(\frac{K_{IC}}{\sigma_Y}\right)^2$$

where σ_Y is the yield stress.

The critical size for a defect may possibly be obtained for ceramic materials where the plastic zone is very small [18] from:

$$a_c = \left(\frac{K_{IC}}{\sigma}\right)^2 \frac{1}{1.21\pi}.$$

For materials as brittle and strong as WC–Co it is preferable to use the analytical method rather than the compliance method [19] or the work-of-fracture method [20], because these last two methods require a knowledge of the displacement ϵ_r of the load F_r. This displacement is very small (10 to 40 μm) and hence very difficult to measure accurately. Some measurements have, however, been made using these methods and the results

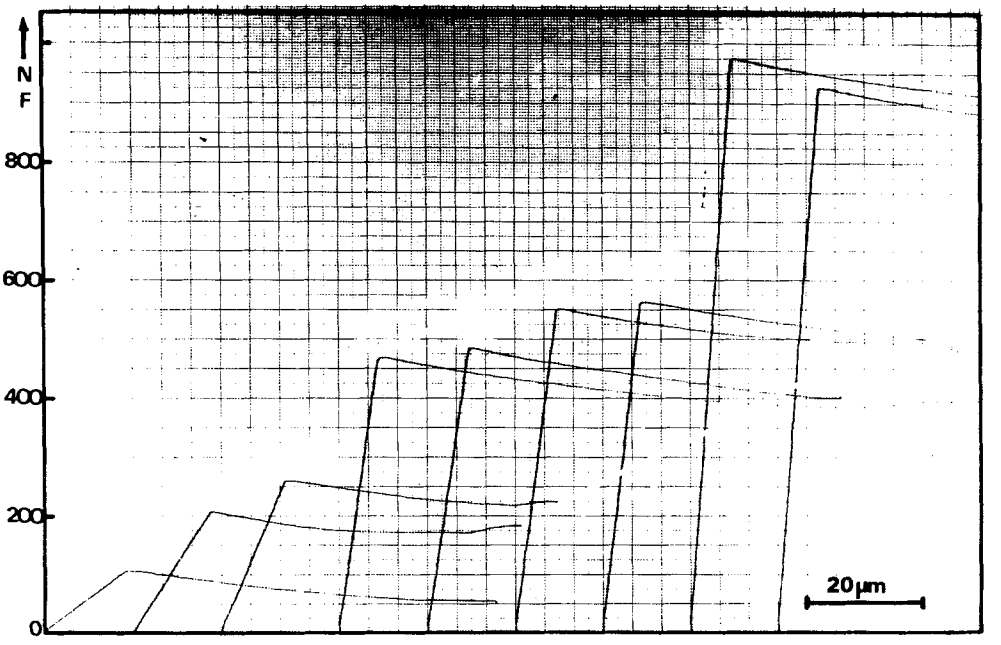

Figure 2 Experimental curves load–displacement for notched specimens: WC–10 wt % Co, $\bar{D}_{WC} = 0.7\ \mu m$.

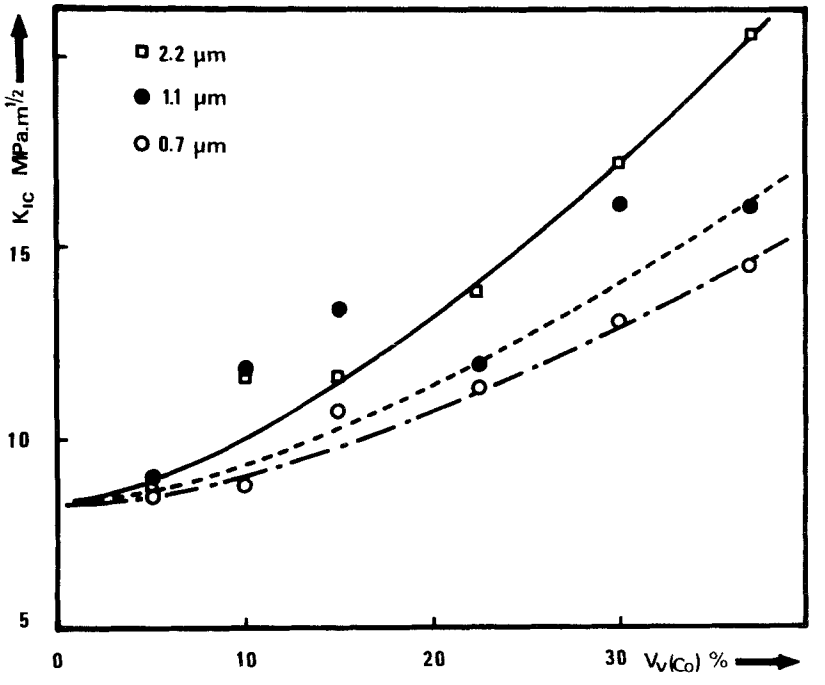

Figure 3 Variation of K_{IC} with the volume fraction of cobalt.

are in agreement with those of the analytical method [21].

The limits of elasticity, σ_Y, were determined in compression with cylindrical specimens 5 mm diameter and 13 mm long and the stress–strain curves were obtained point by point. The permanent deformation of the specimen was measured using a comparator to 1/1000 mm. We have chosen as the yield point a strain of 0.05% plastic deformation because values greater than this change the structure too much to be representative, and furthermore prevent one obtaining a value for the

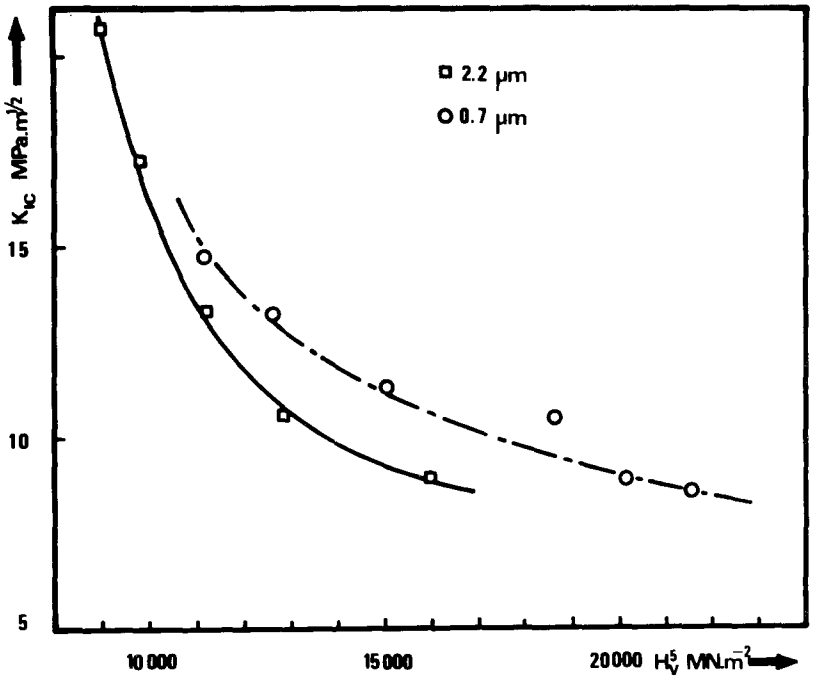

Figure 4 Variation of K_{IC} with the Vickers hardness under a load of 5 kg.

materials with low volume fractions of cobalt.

The rupture stress, σ_r, and Young's modulus, E, were obtained in three-point bending on polished specimens 200 mm × 5 mm × 1 mm, the distance between the lower knife edges being 16 mm [21, 22]. The hardness was measured with a Vickers diamond under a load of 5 kg (Zwick apparatus).

The abrasive wear tests were carried out by Ugine–Carbone on a Fargo machine by rubbing the specimen (39 mm × 23 mm × 8 mm) (5, 10, 15 and 30 Co vol %) with wet brown alumina AS O SB 15, grain size 30 (300 to 1500 μm) from Pechiney, under a load of 20 kg for 1300 cycles (100 rev min^{-1}).

3. Results

3.1. Variation of K_{IC} as a function of simple microstructural parameters

The dependence of K_{IC} on the volume fraction of cobalt is given in Fig. 3. For a given grain size a steady increase of K_{IC} with increasing volume fraction of cobalt $V_{V(Co)}$ is observed. This is expected because if the critical stress intensity factor represents the resistance to crack propagation, its value must increase with the ductility of the material. The influence of the mean diameter of the carbide crystals appears to be more marked when the volume fraction of cobalt increases, and it is the materials with the coarsest grain sizes which are the toughest. The critical values of the strain energy release rate, G_{IC}, varies in the same way as K_{IC}. These results are in good agreement with those of other authors [1, 4, 6, 7]. It is interesting to note that the methods of measurement and the shape of the notches ("V" or "U"), and of the specimens (three-point bending [1–3, 8], double cantilever [1], double torsion [4], compact tension [6]) did not influence the value of K_{IC}. Furthermore, some materials from different sources, but with the same microstructural parameters, have the same values of K_{IC}.

3.2. Correlation with some other mechanical parameters

A correlation has been looked for between K_{IC} and mechanical parameters which show a systematic variation as a function of the different microstructural parameters. Amongst the properties look at, hardness values gave the best results. The variation of K_{IC} as a function of the hardness is shown in Fig. 4. The decrease of K_{IC} with hardness was forseeable: the harder a material the more brittle it is. It can be stated, however, that the hardness is still sensitive to the mean diameter of the tungsten carbide crystals. For a given hardness it is the material with the smallest grain sizes which is the toughest.

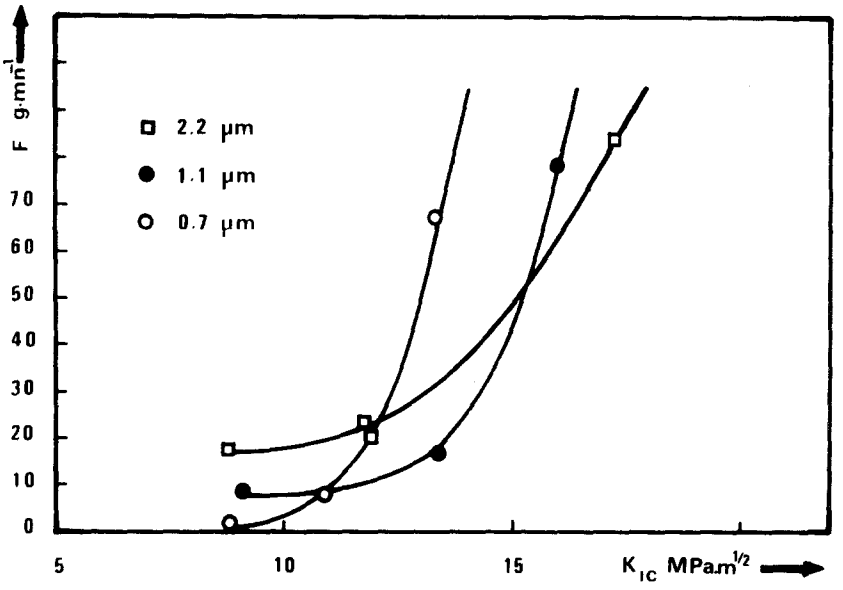

Figure 5 Variation of the loss in weight of the specimens per minute of revolutions of the abrading disc with K_{IC}.

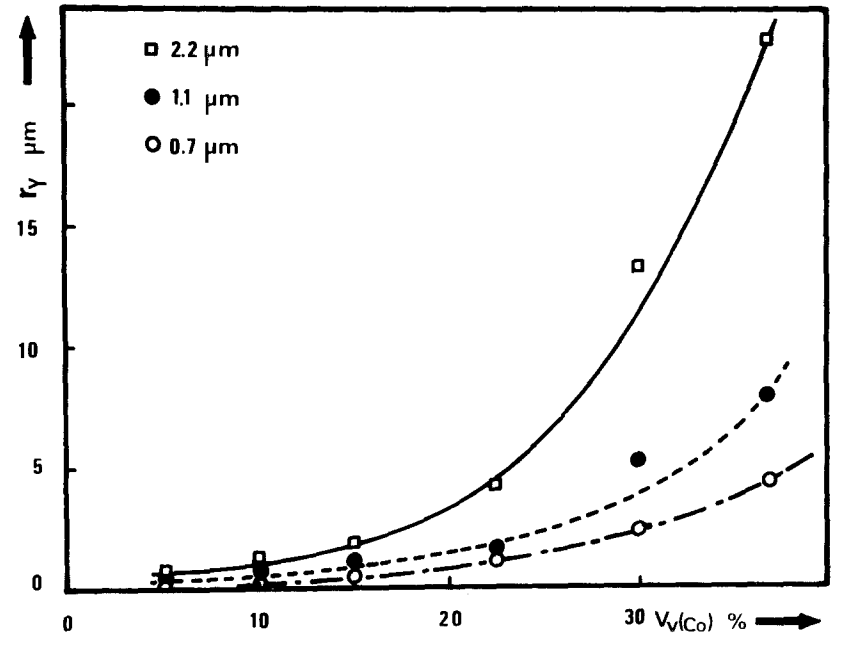

Figure 6 Variation of the radius of the plastic zone, r_Y, with the volume fraction of cobalt.

A study has similarly been made of the relationship between K_{IC} and the abrasive wear resistance. When K_{IC} is plotted against the loss in weight of the specimen per minute, thus $F = \Delta P$/number of revolutions of the abrading disc per minute, it is observed that F increases with K_{IC} (Fig. 5). The material exhibiting most wear is that with the highest volume fraction of cobalt. This is in agreement with the fact that the harder the material, the smaller is K_{IC}, and F is consequently small also.

3.3. Derivation of quantities from K_{IC}

3.3.1. Radius of the plastic zone

It is essential to know the size of the plastic zone in order to confirm that the necessary conditions to obtain the critical values of the stress intensity factor are fulfilled. Furthermore this value has

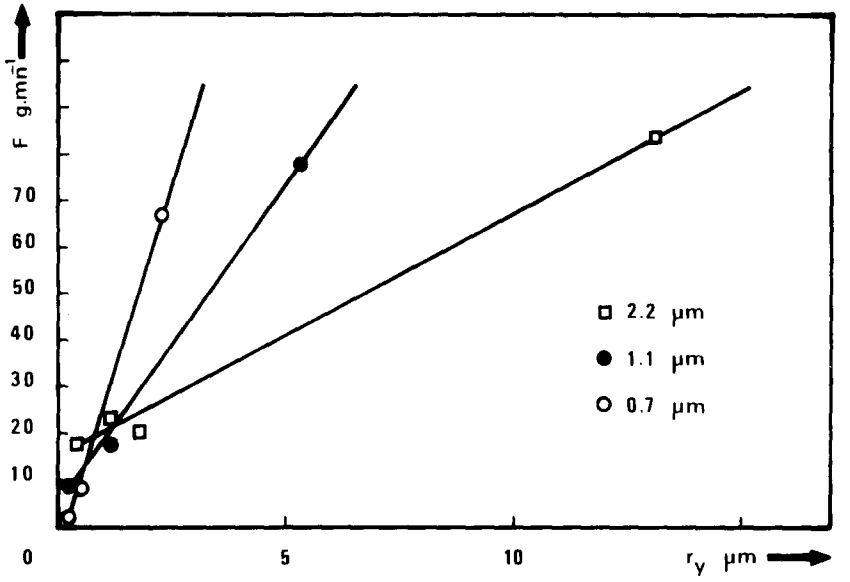

Figure 7 Variation of the loss in weight of the specimen per minute of revolutions of the abrading disc with the radius of the plastic zone size, r_Y.

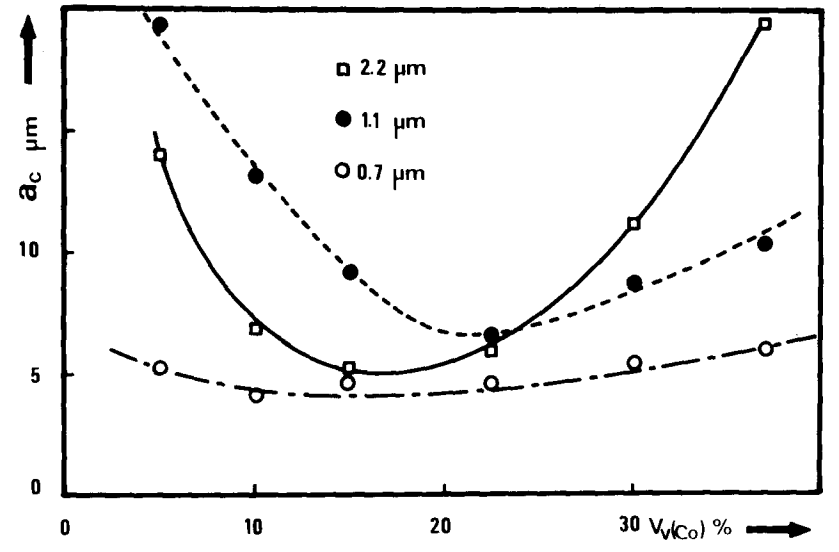

Figure 8 Variation of the critical size defect, a_c, with the volume fraction of cobalt.

already been required to carry out a study of the mechanisms of fracture [4, 8]. We have calculated the radius of the plastic zone using the value of σ_Y 0.05%. The variation of the value of r_Y as a function of the volume fraction of cobalt is represented in Fig. 6. The values obtained are relatively low and it can be said that the necessary conditions are perfectly fulfilled. The radius r_Y increases steadily with the volume fraction of cobalt and is particularly sensitive to the mean diameter of the tungsten carbide crystals.

Moreover, during abrasion, the loss in weight of the specimen per minute, F, is a linear function of the radius of the plastic zone (Fig. 7). It is observed that the smaller this plastic zone is, the lower is the wear, which is consistent with the hardness results. This suggests that the plastic deformation associated with abrasion is responsible for the wear of the material.

3.3.2. Critical size defect

It is useful to know the critical size defect, a_c,

which for a given stress leads to catastrophic fracture. This is particularly important for materials such as WC–Co where the critical size defect is relatively small, given the low values of K_{IC}. We have chosen to determine the critical size for a semi elliptical crack, i.e. Griffith, corresponding to a nominal stress equal to the stress at rupture in bending un-notched specimens using the values given in Table I.

The variation of a_c with the volume fraction of cobalt is shown in Fig. 8. The first comment is that the values are very small and of the same size as only a few carbide crystals. There exists a very marked minimum for the two largest mean grain sizes ($\bar{D}_{WC} = 2.2$ and $1.1\,\mu m$), and at compositions which correspond to the maxima values of the rupture stress. Furthermore it should be noted that the size of critical defect varies very little with the volume fraction of cobalt for specimens of small mean grain size ($\bar{D}_{WC} = 0.7\,\mu m$).

3.4. Analysis of the fracture

A preliminary study demonstrated that the methods of quantitative metallography and stereology can be applied to a study of the rupture of materials [23, 24]. We have, therefore, analysed statistically the fracture path on the face of the crack propagation, bearing in mind the different types of fracture in WC–Co composites: fracture of the carbide crystals designated W/C, fracture following the interface of the carbide crystals designated WC/WC, fracture following the interface carbide–cobalt designated WC/Co, and finally the rupture of the cobalt phase designated Co/Co (Fig. 9). To do this we have considered, on the one hand, the mean distance covered by each of the four fracture modes (Fig. 10) and, on the other hand, their relative participation (Fig. 11).

The mean distance of fracture in the carbide phase, $\overline{W/C}$ and $\overline{WC/WC}$, is constant and essentially of the same magnitude as the mean diameter of tungsten carbide crystals. The mean distance traversed in the cobalt phase, $\overline{WC/Co}$ and $\overline{Co/Co}$, increases regularly with the volume fraction of cobalt and approaches a limiting value close to the diameter of the tungsten carbide crystals of the different specimens.

As regards the relative proportion of each type of fracture (Fig. 11 and Table II), it can be observed that the most important mode is fracture following the interface WC/WC and it decreases with increasing cobalt content. Furthermore, this variation is almost coincident with that for the carbide phase. The amount of transgranular fracture in the carbide crystals passes through a maximum, whereas the proportion in the cobalt,

TABLE I The characteristics of the WC–Co materials studied: $\bar{D}_{WC}$, mean diameter of tungsten carbide crystals; $V_{V(Co)}$, cobalt volume fraction; E, Young modulus; σ_Y, yield point at 0.05%; σ_r, rupture stress by bending; K_{IC}, critical stress intensity fractor; G_{IC}, critical value of the strain energy release rate; a_c critical size defect; r_y, radius of plastic zone. The values presented are averaged over 25 to 40 measurements, except for $\sigma_Y = 0.05\%$ (5 measurements).

$\bar{D}_{WC}$ (μm)	$V_{V(Co)}$ (%)	E ($MN\,m^{-2}$)	$\sigma_Y = 0.05\%$ ($MN\,m^{-2}$)	σ_r ($MN\,m^{-2}$)	K_{IC} ($MPa\,m^{-1/2}$)	G_{IC} ($J\,m^{-2}$)	a_c (m)	r_Y (μm)
2.2	5	643 600	2900	1200	8.8	115	14.0	0.5
	10	613 400	2450	2300	11.8	215	6.9	1.2
	15	570 000	2000	2700	11.9	236	5.0	1.8
	22	485 000	1500	2800	13.5	347	6.1	4.2
	30	447 000	1100	2650	17.3	644	11.2	13.1
	37	421 000	1000	2500	20.7	991	19.6	22.7
1.1	5	645 000	3800	1060	9.1	124	19.6	0.3
	10	610 500	3200	1690	11.9	219	13.0	0.7
	15	570 000	2800	2280	13.4	304	9.1	1.2
	22	493 000	2200	2530	12.0	276	5.9	1.6
	30	447 000	1600	2750	16.0	549	8.9	5.3
	37	415 000	1400	1670	16.0	592	10.2	7.9
0.7	5	645 000	4800	1940	8.8	114	5.2	0.2
	10	629 000	4000	2250	8.8	120	4.0	0.3
	15	570 000	3400	2500	10.9	200	5.0	0.5
	22	505 000	2600	2700	11.4	252	4.7	1.0
	30	447 000	2000	2910	13.3	379	5.5	2.3
	37	408 200	1600	3090	14.5	486	5.8	4.3

TABLE II Characteristics of fracture: types of fracture observed on the face of the crack propagation for a notched specimen of WC–Co, $\bar{D}_{WC}$ 2.2 μm with: $V_{V(Co)}$, volume fraction cobalt; $\overline{W/C}$, mean distance of fracture in transgranular rupture in tungsten carbide, W/C; $\overline{WC/WC}$, mean distance of fracture in the interface WC/WC; $\overline{WC/Co}$, mean distance of fracture in the interface WC/Co; $\overline{Co/Co}$, mean distance of fracture in transgranular rupture in cobalt, Co/Co.

$V_{V(Co)}$ (%)	Fracture transgranular W/C		Fracture interfacial WC/WC		Fracture interfacial WC/Co		Fracture transgranular Co/Co	
	(%)	$\overline{W/C}$ (μm)	(%)	$\overline{WC/WC}$ (μm)	(%)	$\overline{WC/Co}$ (μm)	(%)	$\overline{Co/Co}$ (μm)
5	25.5	2.76	69.0	2.09	5.4	0.97	–	–
10	33.7	2.92	59.1	2.19	6.9	1.17	0.35	1.03
15	31.8	2.73	46.2	2.07	18.8	1.40	3.20	1.04
22	27.5	2.36	46.7	2.07	20.9	1.51	4.74	1.34
30	30.0	2.40	41.7	2.05	23.8	1.63	4.00	1.41
37	16.5	2.65	34.6	2.11	35.6	1.94	13.40	1.65

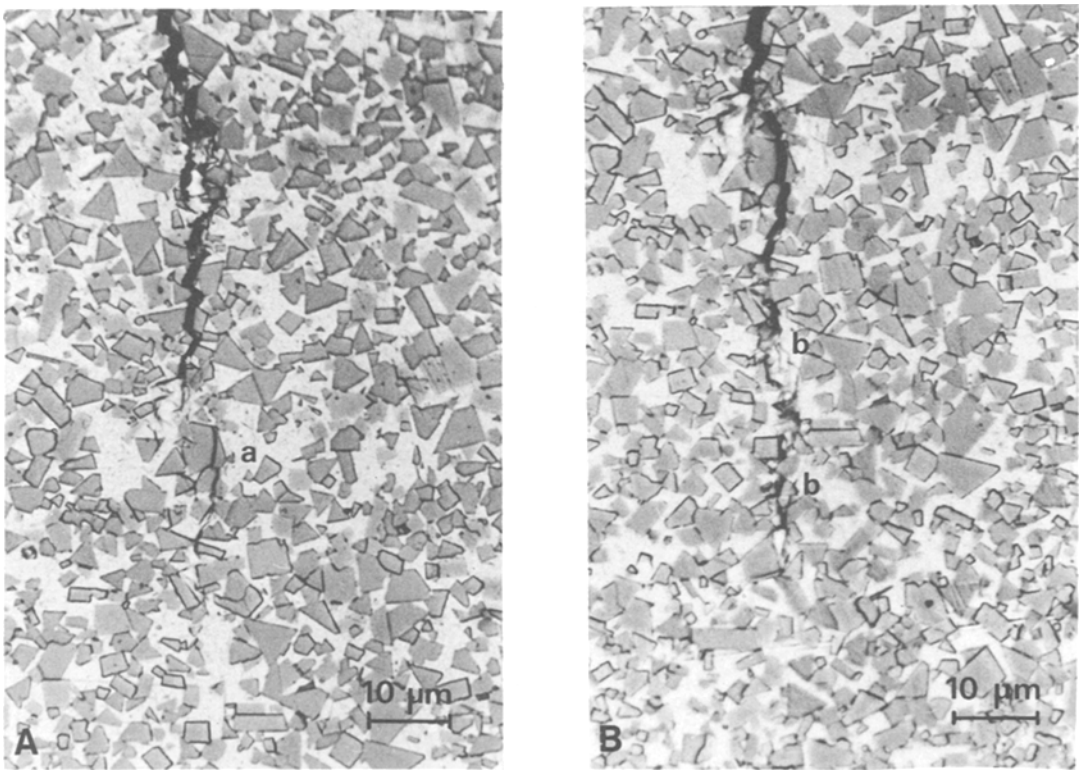

Figure 9 Propagation of a crack in WC–25 wt % Co, $\bar{D}_{WC} = 2.2\,\mu m$, illustrated by two micrographs of the same region.

WC/Co and Co/Co, is of relatively minor importance for the lower volume fractions of cobalt, but becomes much more important for higher volume fractions. In addition, the fraction of rupture occurring essentially in the carbide phase, WC/WC + W/C, follows the carbide volume fraction measured in the bulk material.

4. Discussion

To formulate a mechanism for the crack propagation, it is necessary to investigate the correlation between toughness parameters and microstructural characteristics. The mean free path in the cobalt phase, $\bar{L}_{Co}$, has already provided very good correlation particularly for the limit of elasticity [21, 25] as well as for the fracture toughness [8]. The variation of K_{IC} with the mean free path in the cobalt phase is represented in Fig. 12. It can be seen that for a given grain size K_{IC} is a linear function of $\bar{L}_{Co}$. However, the extrapolation of

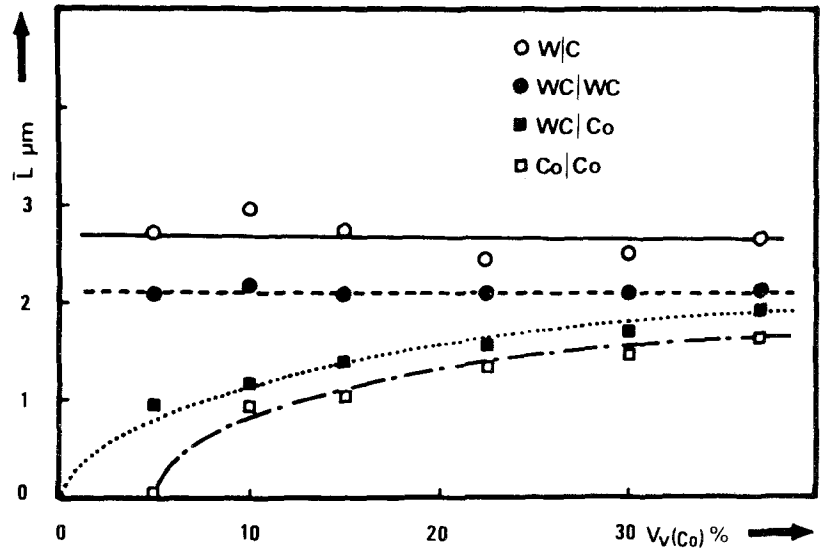

Figure 10 Mean distance travelled over the fracture path for each type of fracture on the face of the crack propagation of a notched specimen as a function of the cobalt content for WC–Co composites of $\bar{D}_{WC} = 2.2\,\mu m$.

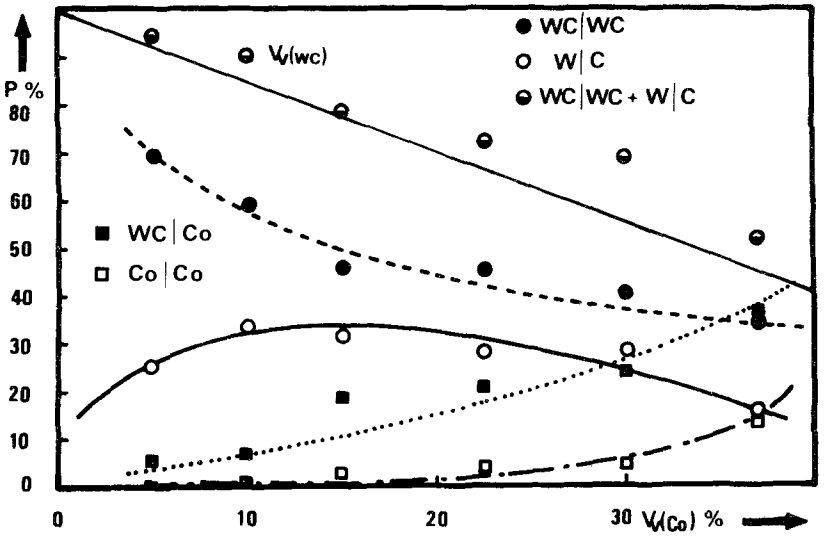

Figure 11 Variation of the porportion of each type of fracture on the face of the crack propagation for a notched specimen as a function of the volume fraction of cobalt for WC–Co materials with $\bar{D}_{WC} = 2.2\,\mu m$.

K_{IC} to zero $\bar{L}_{Co}$ does not provide a unique value of K_{IC} for pure carbide, as is the case when plotted against $V_{C(Co)}$. This could result from the fact that for very low cobalt compositions, the mean free path in the cobalt phase is no longer a good microstructural parameter to describe the microstructure at low cobalt volume fractions. It is interesting to note that in this case, for the range of mean grain size studied, a linear relationship is obtained between K_{IC} and $\bar{D}_{WC}^{-1/2}$ for constant mean free path in the cobalt phase (Fig. 13).

We have investigated new relationships between K_{IC} or similar quantities and other microstructural parameters such as contiguity C_{WC} or dimensionless parameters such as $\bar{L}_{Co}/\bar{D}_{WC}$. In Fig. 14 the variation of K_{IC} is given as a function of contiguity in the carbide phase. In the range of cobalt volume fractions studied it appears that K_{IC} is a unique function of C_{WC}. It can be deduced from this that the fracture toughness of the tungsten carbide cobalt materials is determined by the area of contacts between the carbide crystals and, therefore,

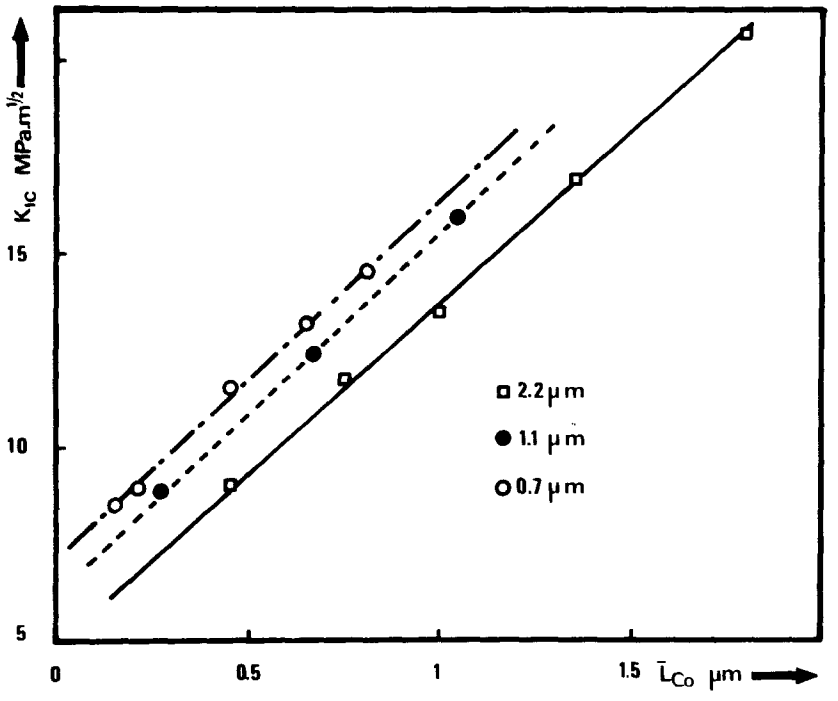

Figure 12 Variation of K_{IC} with the mean free path in the cobalt phase, $\bar{L}_{Co}$.

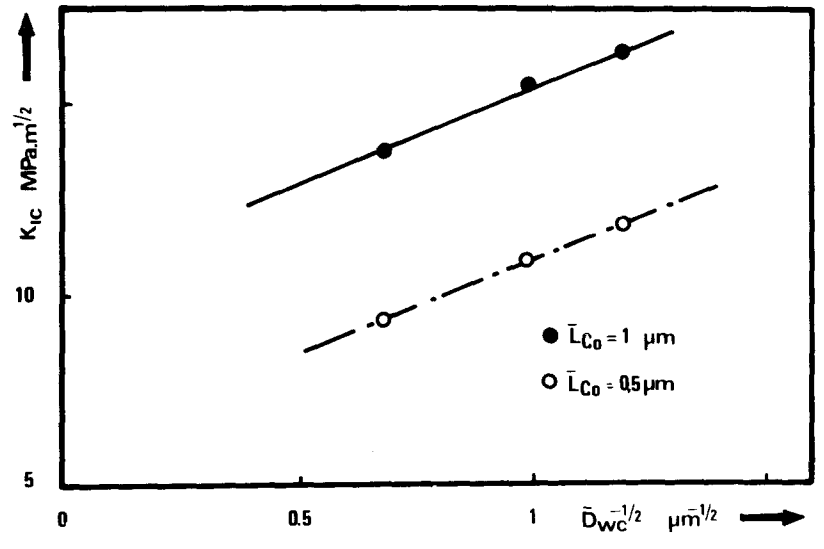

Figure 13 Variation of K_{IC} with $\bar{D}_{WC}^{-1/2}$, for a constant mean free path in the cobalt phase.

by the ease that the crack can propagate in the most brittle phase of compounds of this type.

The metallographic analysis of crack propagation permits the conclusion to be drawn that the crack advances in several stages [8, 22] (Fig. 9): there is first statistical fracture of carbide crystals in front of the crack (Fig. 9A, region a); these localized fractures afterwards join up at the root of the crack either by intergranular debonding or by rupture of the cobalt phase (Fig. 9B, region b). The distance between the isolated fractured crystals and the root of the crack and the proportion of fracture inter- or transgranular, appears to be related to the size of the plastic deformation zone and tungsten carbide crystals.

It appears that in the case of fracture of

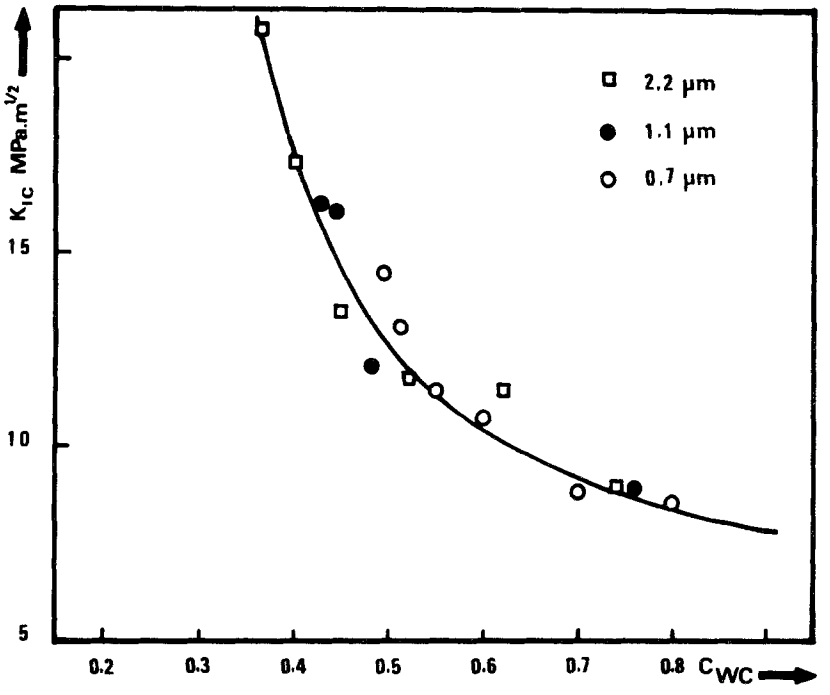

Figure 14 Variation of K_{IC} with the contiguity of the carbide phase, C_{WC}.

WC–Co, the plastic deformation of the cobalt phase plays an important role [21]. Gurland [26] and Nabarro and Luyckx [27], proposed a model of fracture of WC–Co, according to which the fracture of the carbide crystals is due to the plastic flow of cobalt. Thus it would appear that the parameter $\bar{L}^2_{Co}/\bar{D}_{WC}$ is very important, because it takes account of the size of the cobalt regions and of the mean diameter of carbide crystals. In addition it has the dimensions of length which avoids meaningless extrapolations. This parameter is justified as follows: the strain energy of a dislocation pile-up of unit length is of the form $n^2\mu b^2$ (n is the number of dislocations, μ the shear modulus, and b the Burgers vector). Now n is proportional for a given stress to the length of the pile-up. Under these conditions the energy of a pile-up is proportional to the square of its length which one can take as equal to the mean size of the cobalt regions, i.e. in effect the mean free path in the cobalt phase $\bar{L}_{Co}$. This energy is thus of the form:

$$W = n^2\mu b^2 = A\bar{L}^2_{Co}. \quad (1)$$

At the instant of the opening of the crack in the tungsten carbide crystal this strain energy is converted to surface energy, hence [26]:

$$n^2\mu b^2 = 2\gamma\bar{D}_{WC}. \quad (2)$$

The conditions of the fracture of WC are therefore given by the morphological parameter $\bar{L}^2_{Co}/\bar{D}_{WC}$ as a result of the equality of Equations 1 and 2. Gurland, when discussing the mechanical properties of sintered tungsten carbide–cobalt alloys, prefered to describe the relation in terms of $F^{2/3}/\bar{D}_{WC}$ (F is the volume fraction of tungsten carbide), in order to emphasize the analogy with the strain-hardening mechanism due to dispersions, proposed by Fisher *et al.* [28]. However, since the mechanism is more applicable to alloys with low carbide content, it appears to us more appropriate to use the parameters $\bar{L}_{Co}$ and $\bar{D}_{WC}$ which are more representative of the microstructure.

If the fracture ahead of the carbide crystals is due to the plastic flow of cobalt, we can obtain a simple relationship between $\bar{L}^2_{Co}/\bar{D}_{WC}$ and G_{IC}, which describes the work-hardening in the plastic zone when the crack advances. It can be seen in Fig. 15 that G_{IC} is a unique linear function of $\bar{L}^2_{Co}/\bar{D}_{WC}$. This results from the above analysis. It appears that the crack propagation in the WC–Co materials is determined by the plastic flow of cobalt which causes the fracture of the carbide crystals ahead of the crack.

5. Conclusions

The values of the critical stress intensity factor and the parameters which are dependent on it

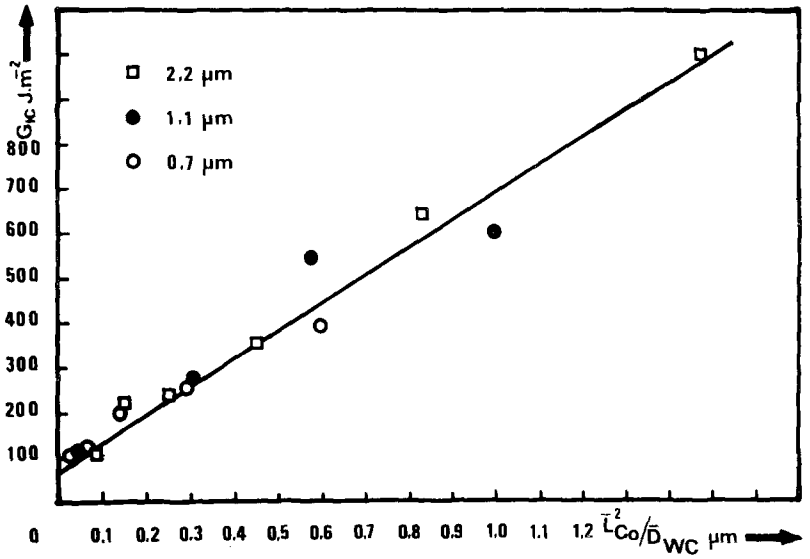

Figure 15 Variation of G_{IC} with $\bar{L}^2_{Co}/\bar{D}_{WC}$.

have been measured for a wide range of volume fractions of cobalt and for several carbide grain sizes. The study of the dependence of these values as a function of the microstructural parameters leads to two important conclusions: firstly K_{IC} is a unique function of the contiguity of the carbide phase, which is supported by the role played in fracture of the joints between tungsten carbide crystals; secondly the variation of G_{IC} as a function of $\bar{L}^2_{Co}/\bar{D}_{WC}$ shows the role played by the plastic deformation of cobalt and the relative dimensions of the carbide and cobalt phases. The analysis of the results, as well as the fracture path, has enabled a tentative fracture mechanism for these materials to be formulated.

Acknowledgements

The authors would like to thank Professor A. Deschanvres for his helpful discussions, Dr B. L. Mordike for critically reading the manuscript and improving the English, and Ugine–Carbone for the measurements of the abrasive wear resistance. This investigation was supported by the Délégation Générale à la Recherche Scientifique et Technique, contrat no. 74.7.1075.

References

1. S. S. YEN, M.S. Thesis, Lehigh University (1971).
2. J. L. CHERMANT, A. DESCHANVRES and A. IOST, *Mat. Res. Bull.* 8 (1973) 925.
3. *Idem*; in "Fracture Mechanics of Ceramics", edited by R. C. Bradt, D. P. H. Hasselman and E. F. Lange, (Plenum Press, New York, 1974) p. 347.
4. R. C. LUETH, *ibid*, Vol. II (1974) p. 791.
5. F. OSTERSTOCK, Diplôme d'Etudes Approfondies, Caen (1974).
6. N. INGELSTRÖM and H. NORDBERG, *Eng. Fract. Mech.* 6 (1974) 597.
7. T. JOHANNESSON, 4th European Symposium for Powder Metallurgy, Grenoble, 13–15 May 1975, no. 5–11.
8. J. L. CHERMANT, F. OSTERSTOCK and R. MEYER, *ibid*, no. 5–12.
9. S. A. SALTYKOV, "Stereometric Metallography" (Metallurgizdat, Moscow, 1958).
10. M. COSTER, Thèse de Doctorat ès-Sciences, Caen, (1974).
11. M. DROUZY, *Prakt. Metal.* 9 (1967) 481.
12. Proposed recommended practice for plane-strain fracture toughness testing of high-strength metallic materials using a fatigue-cracked bend specimen, *A.S.T.M. Standards* 31 (1968) 1018.
13. Norme A.F.N.O.R., A 03-180, (February 1974).
14. W. F. BROWN and J. E. SRAWLEY, A.S.T.M.-S.T.P. 410 (1967).
15. R. P. FELGAR and J. D. LUBAHN, *Trans. Soc. Test. Mat.* 57 (1957) 770.
16. H. DOI, Y. FUJIWARA, K. MIKAYE and Y. OOSAWA, *Met. Trans.* 1 (1970) 1417.
17. G. R. IRWIN, *J. Appl. Mech.* 24 (1957) 361.
18. R. PABST, *Z. Werkstofftechnik* 6 (1975) 17.
19. R. W. DAVIDGE and G. TAPPIN, *J. Mater. Sci.* 3 (1968) 165.
20. J. NAKAYAMA, *J. Amer. Ceram. Soc.* 48 (1965) 583.
21. F. OSTERSTOCK, Thèse d'Ingénieur Docteur, Caen, (1975).
22. J. L. CHERMANT, A. IOST and F. OSTERSTOCK, *Proc. Brit. Ceram. Soc.* 25 (1975) 197.
23. J. L. CHERMANT, M. COSTER and A. DESCHANVRES, *Metallogr.* 8 (1975) 271.
24. *Idem, ibid* 9 (1976) 199.

25. H. DOI, Y. FUJIWARA and Y. OOSAWA, Proceedings of the International Conference on Mechanical Behavior of Materials, Vol. V (The Society of Materials Sciences, Japan, 1972) p. 207.
26. J. GURLAND, *Trans. Met. Soc. AIME* **227** (1963) 1146.
27. F. R. N. NABARRO and S. B. LUYCKX, *Trans. J. Inst. Met.* 9 suppl. (1968) 610.
28. J. C. FISHER, E. W. HART, R. H. PRY, *Acta Met.* 1 (1953) 336.

Received 11 November 1975 and accepted 19 March 1976.